Nucleic Acids Research, 2017 **1**
doi: 10.1093/nar/gkx195

Critical 23S rRNA interactions for macrolide-dependent ribosome stalling on the ErmCL nascent peptide chain

Miriam Koch[1], Jessica Willi[1], Ugo Pradère[2], Jonathan Hall[2] and Norbert Polacek[1,*]

[1]Department of Chemistry and Biochemistry, University of Bern, Freiestrasse 3, 3012 Bern, Switzerland and [2]Institute of Pharmaceutical Sciences, Department of Chemistry and Applied Biosciences, ETH Zurich, 8093 Zurich, Switzerland

Received December 22, 2016; Revised March 09, 2017; Editorial Decision March 11, 2017; Accepted March 14, 2017

ABSTRACT

The nascent peptide exit tunnel has recently been identified as a functional region of ribosomes contributing to translation regulation and co-translational protein folding. Inducible expression of the *erm* resistance genes depends on ribosome stalling at specific codons of an upstream open reading frame in the presence of an exit tunnel-bound macrolide antibiotic. The molecular basis for this translation arrest is still not fully understood. Here, we used a nucleotide analog interference approach to unravel important functional groups on 23S rRNA residues in the ribosomal exit tunnel for ribosome stalling on the ErmC leader peptide. By replacing single nucleobase functional groups or even single atoms we were able to demonstrate the importance of A2062, A2503 and U2586 for drug-dependent ribosome stalling. Our data show that the universally conserved A2062 and A2503 are capable of forming a non-Watson–Crick base pair that is critical for sensing and transmitting the stalling signal from the exit tunnel back to the peptidyl transferase center of the ribosome. The nucleobases of A2062, A2503 as well as U2586 do not contribute significantly to the overall mechanism of protein biosynthesis, yet their elaborate role for co-translational monitoring of nascent peptide chains inside the exit tunnel can explain their evolutionary conservation.

INTRODUCTION

The ribosome is a gigantic macromolecular machine translating the information encoded on a messenger RNA (mRNA) into a polypeptide sequence by the sequential addition of single amino acids. Peptide bond formation is catalyzed in the peptidyl transferase center (PTC), which is located in a cleft on the intersubunit side of the large ribosomal subunit (1–3). In order to leave the ribosome and enter into the cytosol, a newly synthesized polypeptide chain passes through the ribosomal exit tunnel. This tunnel has a diameter of 10–20 Å and a length of ∼100 Å and spans the whole large ribosomal subunit. The ribosomal exit tunnel is mainly composed of ribosomal RNA (rRNA), as shown by X-ray structures of the bacterial and archaeal ribosomes (4–7). The functional role and contribution of the ribosomal exit tunnel to polypeptide synthesis and protein folding is only beginning to be understood in molecular terms. In recent years, it became evident that the tunnel plays an active role in translation regulation and protein folding (reviewed in 8–10). Translation regulation is achieved by specific interactions of the nascent polypeptides with the tunnel wall, resulting in the extreme cases in a programmed translation arrest, the so-called ribosomal stalling.

Ribosomal stalling has been described for several bacterial (e.g. *ermC, ermA, ermB*, *secM, mifM, tnaC*), eukaryal (e.g. the arginine attenuator peptide AAP) as well as for viral (upstream open reading frame of a cytomegalovirus glycoprotein) genes (reviewed in 11). Typically, programmed ribosome stalling in the upstream open reading frame (uORF) is utilized to regulate translation of a downstream ORF. In bacteria programmed translational arrest in the upstream ORF (uORF) results in an upregulation of expression of the downstream gene. This either occurs via transcriptional anti-termination when the stalled ribosome blocks the binding site of the Rho transcription terminator or via inducing a conformation rearrangement in the mRNA structure, thereby exposing the Shine-Dalgarno sequence of the downstream ORF, allowing ribosome binding and therefore translation (11).

One well-characterized and important class of genes regulated by programmed translational arrest are the *erm* genes that encode rRNA methyltransferase enzymes conferring resistance to erythromycin and other macrolide antibiotics

*To whom correspondence should be addressed. Tel: +41 316314320; Email: norbert.polacek@dcb.unibe.ch
Present address: Miriam Koch, The Scripps Research Institute, 130 Scripps Way, Jupiter, FL 33458, USA.

(12). The *ermC* gene is one member of this class and its expression is controlled by an uORF encoding the leader peptide ErmCL (13,14). In the absence of macrolide antibiotics, the ribosome binding site and start codon of *ermC* are sequestered in a stem loop structure and are therefore inaccessible for initiating ribosomes (Figure 1A). However, in the presence of sub-inhibitory concentrations of the macrolide, the ribosome stalls with the isoleucine codon at position 9 (Ile9) of *ermCL* in the P-site. Ribosome stalling induces rearrangements of the mRNA structure thus exposing the ribosome binding site of the downstream ORF allowing the ErmC methyltransferase encoded in *ermC* to be expressed (12). Insights into the molecular mechanism of macrolide-induced ribosome stalling upon synthesis of the ErmC leader peptide have been gained in genetic (14), biochemical (15–17) and structural studies (18). It has been shown that the four C-terminal ErmCL residues $I_6F_7V_8I_9$ are crucial for ribosome stalling and that translation is arrested likely due to the PTC adopting an inactive conformation that prevents peptide bond formation with the incoming Ser-tRNA^{Ser} at the 10th *ermCL* codon position (17). It has been shown that mutations of the universally conserved 23S rRNA nucleotide A2062 and A2503 (*Escherichia coli* nomenclature here and throughout) abolish stalling on the *ermCL* ORF, highlighting a crucial role of these tunnel residues (16). It has been suggested that these two adenosines come into hydrogen bonding distance in the presence of the stalling peptide sequence forming a non-Watson-Crick base pair (3,16,18,19). Notably, mutations of A2062 or A2503 show strictly parallel effect on translation arrest (mutations of both diminish stalling on *ermCL, ermAL1* and *secM*, whereas they do not affect stalling on *ermBL, ermDL* and *tnaC*), suggesting that both adenines may act as components of the same signaling pathway from the tunnel to the PTC (16). Besides these two rRNA residues, the recent cryo-EM structure of the *ermCL* stalled ribosomal complex revealed other 23S rRNA tunnel residues to interact with the ErmCL nascent chain or to adopt a distinct conformation in the stalled ribosome suggesting a possible contribution to translation arrest (18). One of these residues is U2506, which interacts with V8 of the ErmCL nascent polypeptide chain and seems to stack upon the aromatic side chain of F7. Both V8 and F7 belong to the ErmCL amino acids ($I_6F_7V_8I_9$) crucial for stalling (17). The same might be true for U2586 that interacts with I6 of the ErmCL nascent chain. Mutation of U2586 to either A, C or G did not affect wildtype *ermCL* stalling, whereas the arrest efficiency of *ermCL*-I6A could be partially rescued by these mutations (18). Furthermore, the structure also revealed an interaction of the ErmCL critical $I_6F_7V_8I_9$ sequence with A2062 thus supporting a steric role of the N-terminus for ribosome stalling (17).

To gain molecular insight into the contribution and specific interactions of distinct 23S rRNA residues to macrolide-induced ribosome stalling upon synthesis of ErmCL, we are using the atomic mutagenesis approach (20–22). This experimental approach allows the introduction of non-natural nucleoside analogs into the 23S rRNA in the context of functional 70S ribosomes. By this technique single functional group or even single atom substitutions of 23S rRNA residues are possible. To identify the 23S rRNA functional groups and interactions that are involved in sensing the arrest peptide and possibly transmitting the signal to the PTC, we targeted the 'main suspects' for ErmCL stalling, namely A2062, U2503, U2506, U2585, U2586 and A2602 by this nucleotide analogue interference approach.

MATERIALS AND METHODS

Reconstitution of 50S subunits

Generation of the circularly permuted (cp) 23S rRNA, subsequent *in vitro* reconstitution of the 50S particles from *Thermus aquaticus*, and reassociation with native *E. coli* 30S ribosomal subunits were performed as previously described (20,21,23). Reconstitution reactions contained either 0.5 mM low molecular weight facilitators of the *in vitro* 50S subunit assembly: either RU66252 (stalling) or solithromycin (translation). The presence of macrolide antibiotics positively affect *in vitro* assembly of 50S subunits (24). After reconstitution and association with native 30S *E. coli* subunits, the ribosomal particles are ethanol precipitated and subsequently resuspended directly in the respective reaction buffer (see below). This precipitation step significantly reduces the macrolide concentration initially needed for efficient 50S reconstitution, since no inhibition of downstream functional assays has been observed (20,25,26). Since solithromycin does not trigger *ermCL* stalling (17), whereas RU66252 does, we used the former for 50S reconstitutions employed in subsequent translation control reactions, and the latter for all stalling experiments (see below). Primers used for generation of the different DNA templates for the cp-23S rRNA *in vitro* transcription are listed in Supplementary Table S1. Cp-23S rRNA constructs are named the following way: first number marks the 5′-end of the cp-23S rRNA and the second number indicates the 3′-end (Supplementary Figure S1). During *in vitro* reconstitution of the 50S ribosomal subunit the introduced sequence gap in the cp-23S rRNA encompassing the 23S rRNA residue under investigation, was compensated by chemically synthesized RNA oligonucleotide, containing either the unmodified wild-type sequences or carrying a single nucleoside analog (Supplementary Table S1). Oligoribonucleotides were added in 5-fold molar excess over cp-23S rRNA during 50S *in vitro* reconstitution (20).

Synthetic RNA oligonucleotides

Non-modified RNA strands as well as those containing a ribose-abasic site analog or the 2-pyridone modification were purchased from *Microsynth*. All other oligoribonucleotides were synthesized *via* standard solid-phase synthesis using 2′-*O*-TBDMS phosphoramidites on a 50 nmol scale (27).The dimethylamino group of oligoribonucleotides 2585_DMA-Py and 2586_DMA-Py was introduced using the convertible nucleoside approach as described previously (28,29). For deprotection and cleavage from solid support, samples were treated with 40% aq. dimethylamine for 2.5 h at 40°C. An equal volume of 25% aq. ammonia was then added and temperature was raised to 65°C for 30 min. RNA was desilylated using 1-methyl-2-pyrrolidone (NMP), triethylamine (TEA), and TEA.3HF

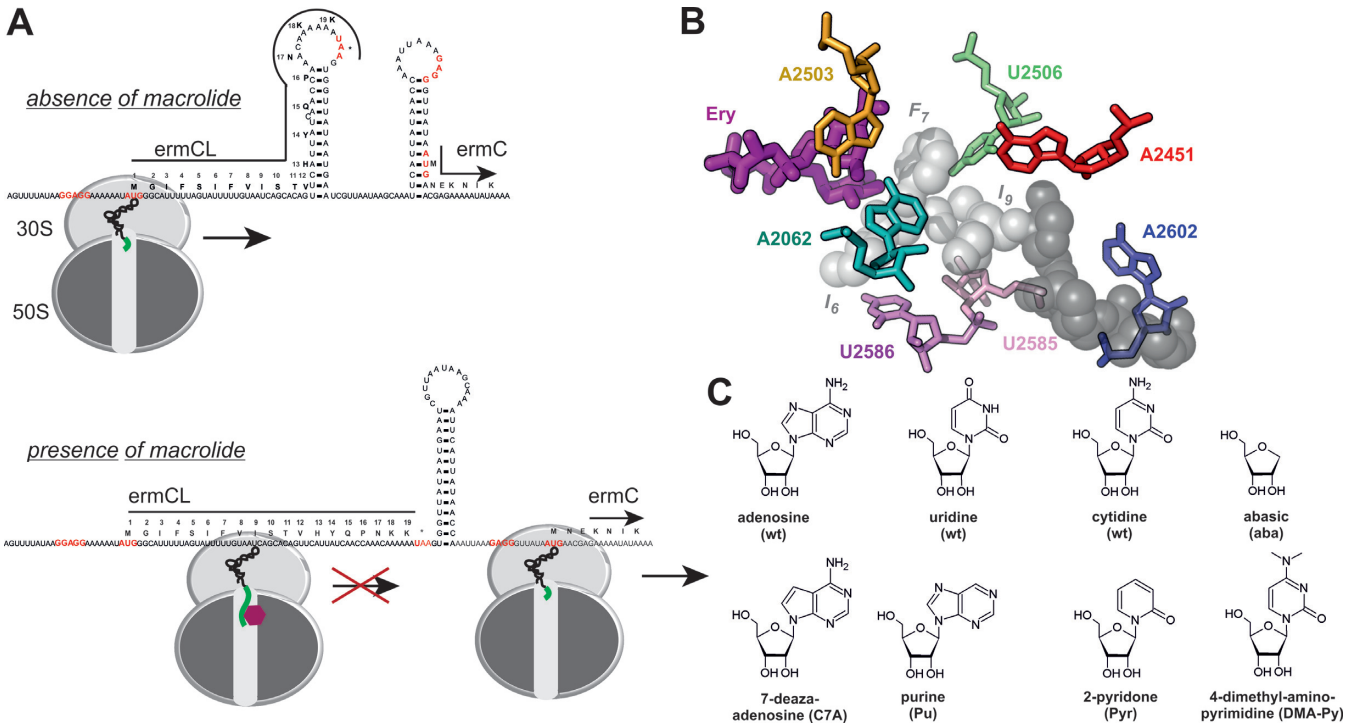

Figure 1. The macrolide-inducible *ermC* gene and the 23S rRNA residues investigated for their role in translation arrest. (**A**) Structure of the regulatory region of the inducible *ermC* gene in the non-induced (upper panel) and induced (lower panel) conformation. The exit tunnel-bound macrolide antibiotic in the large 50S subunit is depicted as purple hexagon and the nascent peptide chain is in green. Amino acid sequence of ErmC leader peptide (ErmCL) and the N-terminus of the ErmC are depicted above the corresponding codons. Shine Dalgarno sequence, start and stop codons are shown in red. (**B**) 3D representation of the PTC and tunnel residues in the ErmCL stalled ribosomal complex (18) (based on the structure pdb 3J7Z) that have been modified and tested for their impact on ribosomal stalling. The PTC residue A2451, whose ribose 2′-OH group is pivotal for peptide bond formation (23,40), is shown as well to indicate the catalytic heart of the active site. The sugar-phosphate backbone of the P-site located peptidyl-tRNA and the density for $I_6F_7V_8I_9$ of ErmCL are depicted in dark and light grey, respectively. Amino acids for which sufficient density was observed in the SRC are labeled in grey. (**C**) The listed nucleoside analogs were introduced via the atomic mutagenesis approach into the PTC or the exit tunnel of the 50S ribosomal subunit and their activities were tested in macrolide-dependent ribosome stalling.

(6:3:4) for 90 min at 70°C. Reaction was quenched using Ethoxytrimethylsilane and samples were purified via HPLC (Agilent 1200 Series; Agilent Technologies) on a C18 column (XBridge OST, particle size 2.5 μm; Waters). Oligoribonucleotides 2503-Purine, 2503-7-deaza-rA, 2062-7-deaza-rA and 2062-Purine were synthesized as above and deprotected in a single step with gaseous methylamine. Oligoribonucleotides were analyzed and confirmed by mass spectrometry (2585_DMA-Py: $Mass_{calc}$ = 9419.8, $Mass_{obs}$ = 9419.2; 2586_DMA-Py: $Mass_{calc}$ = 9420.8, $Mass_{obs}$ = 9420.2; 2503-Purine: $Mass_{calc}$ = 12491.5, $Mass_{obs}$ = 12491.4; 2503-7-deaza-rA: $Mass_{calc}$ = 12505.5, $Mass_{obs}$ = 12504.2; 2062-7-deaza-rA: $Mass_{calc}$ = 8362.1, $Mass_{obs}$ = 8361.4; 2062-Purine: $Mass_{calc}$ = 8348.1, $Mass_{obs}$ = 8348.5).

Toeprint assay

The DNA template for *in vitro* transcription/translation of *ermCL* was amplified via PCR from the pUC18-*ermCLT10*-tandem using 5′-TAATACGACTCACTATAGGG-3′ as forward and 5′-GAACTCATTGTCACTGGTTC-3′ as reverse primer, respectively. The *ermCLT10*-tandem plasmid was generated by cloning the 2x*ermCL* construct (18) into the pUC18 vector via blunt ligation into the SmaI site. The *ermBL* DNA template was generated by PCR using two long overlapping primers. For detection of stalled ribosome complexes by toe-printing, 2 pmol of reconstituted and ethanol precipitated 70S ribosomes were used per *in vitro* translation reaction. *In vitro* translation was performed using the *Δ* ribosomes PURE system (NEB E3312S). The final reaction volume was 5 μl. *In vitro* transcription/translation reactions contained 2 μl solution A, 0.6 μl factor mix, 1 pmol of 5′ ^{32}P-labeled primer (toe-tandem-1: 5′-GAACTCATTGTCACTGGTTC-3′), 8 u RNase inhibitor (ThermoFisher Scientific) and 10 ng of DNA template. The ethanol precipitated reconstituted ribosomes were resuspended in the above translation mixture. The macrolide RU66252 was added to a final concentration of 50 μM, whereas translation control reactions contained 50 μM mupirocin (Ile-tRNA-Synthetase Inhibitor, Sigma Aldrich). All components were combined and the reaction was started by placing the tubes at 37°C. The samples were incubated for 30 min. For cDNA synthesis 1 μl of reverse transcription mixture containing 2 u/μl AMV-RT (Roche, diluted with PSB (9 mM $Mg(OAc)_2$, 5 mM K_3PO_4 pH 7.3, 95 mM potassium glutamate, 5 mM NH_4Cl, 0.5 mM $CaCl_2$, 1 mM spermidine, 8 mM putrescine, 1 mM DTT)) and 2 mM dNTPs were added. Reverse transcription was performed for 10 min at 37°C. Reactions were stopped by addition of 1 μl 10 N NaOH and incubation followed for additional 10 min at 37°C. NaOH was neutralized by

the addition of 0.8 μl HCl (37% (v/v)). Prior to phenol–chloroform–isoamylalcohol (PCI) extraction, 200 μl of resuspension buffer (0.3 M NaOAc pH 5.5, 5 mM EDTA pH 8.0, 0.5% (w/v) SDS) were added to the reactions. After PCI extraction samples were precipitated by the addition of 600 μl ethanol (100% (v/v)) in the presence of 0.5 μl glycoblue (ThermoFisher Scientific) for 30 min at –80°C. After centrifugation (30 min at 18 000 × g, 4°C) pellets were washed with 70% (v/v) ethanol, air-dried and resuspended in 8 μl of loading dye (98% formamide, 5 mM EDTA pH 8.0, 0.1% (w/v) bromphenol blue, 0.1% (w/v) xylene cyanol). Samples were heated up for 1 min at 95°C prior loading on a 6% denaturing 7M Urea polyacrylamide gel (40 cm × 20 cm × 0.375 mm). The gel was run in 1× TBE at 2,000 V, 40 W for 1–1.5 h. The gel was dried on a vacuum dryer for 45 min at 70°C and exposed overnight to a phosphoimager screen.

In vitro translation of ribosomal protein L12 mRNA

In vitro translation of ribosomal protein L12 mRNA using *in vitro* reconstituted ribosomes in the presence of ^{35}S methionine was performed as previously described (20). The radiolabeled reaction products were separated on SDS polyacrylamide gels and detected by phosphorimaging.

Macrolide footprinting

50S reconstitution reactions with 10 pmol cp23S rRNA (cp2596-2566) carrying the compensating synthetic RNA oligonucleotide with either the wildtype or 2-pyridone at position 2586 were set up without macrolides or in the presence of 0.5 mM solithromycin or RU66252, respectively. The chemically engineered 50S subunits were purified by passing them through a 20% sucrose cushion as described (30) and the pellets were resuspended in 20 μl buffer (20 mM Hepes/KOH pH 7.6, 10 mM $MgOAc_2$, 150 mM NH_4Cl, 4 mM 2-mercaptoethanol, 2 mM spermidine, 50 μM spermine) containing 100 μM of either solithromycin or RU66252. Macrolides were allowed to bind to reconstituted 50S or native 50S subunits from *T. aquaticus* for 5 min at 37°C. Dimethylsulfate (1:6 in ethanol, Sigma Aldrich) was added to a final concentration of 100 mM and probing was performed at 37°C for 15 min. Reactions were terminated, rRNA purified and used for reverse transcription as described previously (30,31). For reverse transcription the 5′-^{32}P labeled DNA primer 5′-CATCCTACGCAGGCGC GA-3′ was used and the reaction products were analyzed on a 10% denaturing 7M urea polyacrylamide gel.

RESULTS

Ribosome stalling using *in vitro* reconstituted ribosomes

In order to investigate the role of distinct 23S rRNA residues in macrolide-induced ribosomal stalling on the molecular level, we use the atomic mutagenesis approach (see Figure 1B for a representation of PTC and exit tunnel residues tested). This procedure is based on the *in vitro* assembly of the 50S ribosomal subunit using components from the thermophilic bacteria *T. aquaticus* (20,21,32). We first established the experimental system by analyzing if *in vitro* translation of the arrest peptide ErmCL and macrolide-dependent ribosome stalling could be reproduced using native as well as *in vitro* reconstituted 50S subunits from *T. aquaticus*. We employed purified native 50S subunits from *T. aquaticus* as well as reconstituted 50S containing *in vitro* 23S rRNA transcripts in combination with native *E. coli* 30S for ribosome stalling in presence of the macrolide RU66252. In the presence of this macrolide native ribosomes stall at the ninth codon of *ermCL* with the Ile9-tRNA in the P-site (Figure 1A). Such stalling events can be detected using the inhibition of primer extension (toeprint) as readout (17). Similar to the *E. coli* system, ribosomes with *T. aquaticus* 50S subunits (native as well as *in vitro* assembled) stall efficiently in the presence of the macrolide antibiotic RU66252 as reflected by the specific toeprint band (Figure 2A,C). Importantly this toeprint band only appears in the presence of RU66252 confirming a drug-specific translation arrest in the presence of this macrolide antibiotic. We noticed an increased toeprinting signal at the AUG start codon of *ermCL* in case of employing hybrid ribosomes consisting of native *E. coli* 30S subunits and native or reconstituted *T. aquaticus* 50S subunits compared to experiments with *E. coli* 70S ribosomes (Supplementary Figure S2A). This indicates reduced activity of the hybrid ribosomes during the transition from the initiation to the elongation phase of protein biosynthesis. In the absence of any translation this start codon toeprint disappears and solely a primer extension stop around the stop codon remains which is indicative of an mRNA secondary structure-dependent reverse transcriptase stop (Supplementary Figure S2B).

A2602 in the PTC is not required for drug dependent translation arrest

To investigate the role of the highly flexible 23S rRNA nucleotide A2602, which was found in a distinct conformation in the ErmCL stalled ribosomal complex (SRC) compared to empty ribosomes (18), we *in vitro* reconstituted ribosomes lacking this nucleotide. A2602 is universally conserved, bulges out of 23S rRNA helix 93 (Supplementary Figure S1) and could potentially contribute to ribosome stalling based on its conformational flexibility. Ribosomes lacking A2602 have been shown before to be fully active in *in vitro* translation (25), however are defective in release factor-mediated peptidyl-tRNA hydrolysis (33,34). In order to confirm the translational activity of reconstituted ribosomes in the toeprint assay, mupirocin, an inhibitor of Ile-tRNA-synthetase, was added. The presence of mupirocin leads to the depletion of Ile-tRNA^{Ile} in the translation reaction resulting in an accumulation of ribosomal complexes with an Ile codon in the A-site. The corresponding translation arrest is reflected by the toeprint bands at codon positions 3 and 6 (Figure 2B), thereby confirming the capability of the mutant *in vitro* reconstituted ribosomes for translating the *ermCL* template. In the presence of RU66252, ribosomes lacking A2602 could nevertheless efficiently stall with the lle9-peptidyl tRNA in the P-site (Figure 2B). These results thus demonstrate that A2602 is not involved in the macrolide-dependent programmed translational arrest at the *ermCL* gene. We noticed increased primer extension stops around the stop codon when using ribosomes lacking

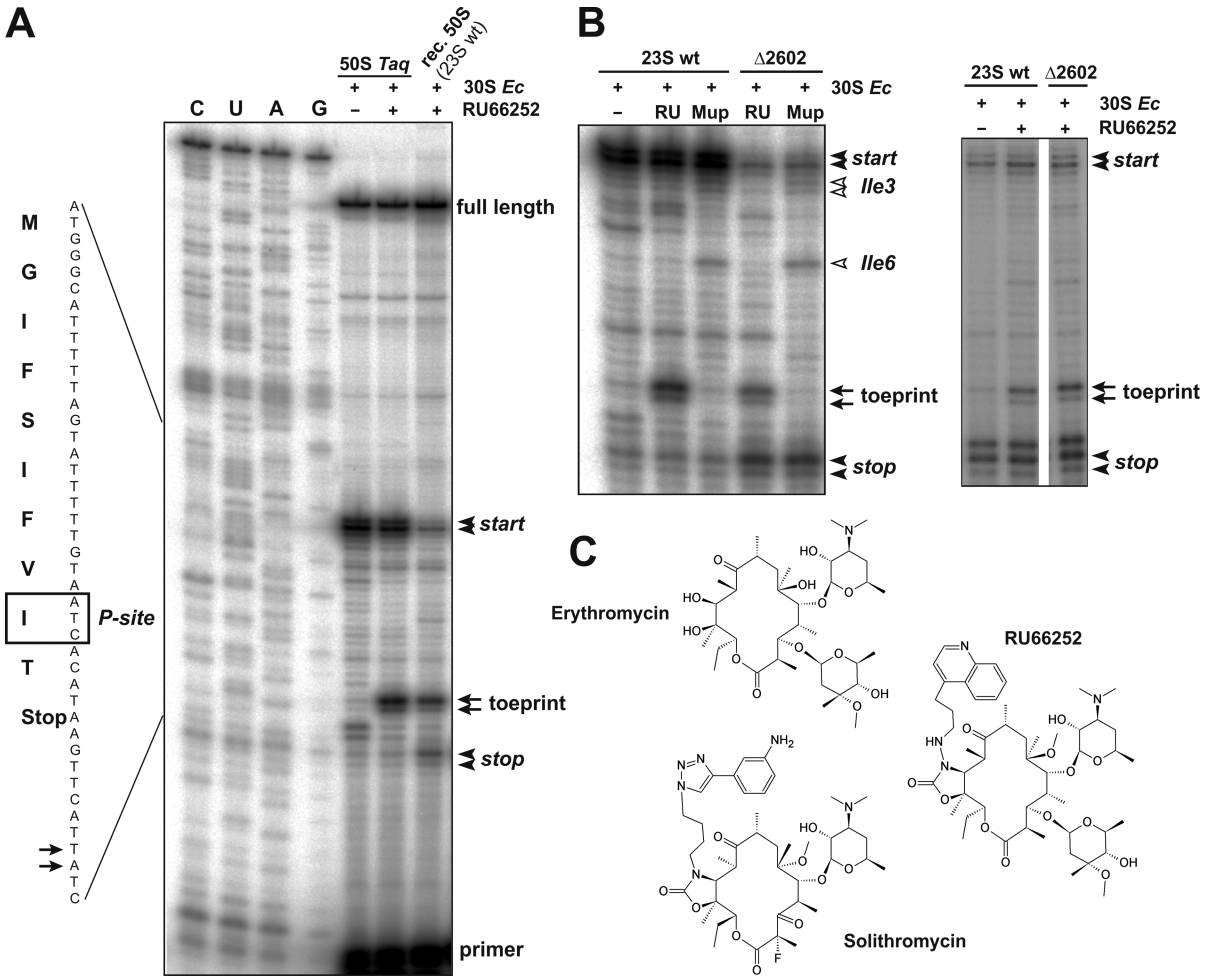

Figure 2. *In vitro* reconstituted ribosomes efficiently stall in the presence of a macrolide on *ermCL*. (**A**) Comparison of native hybrid ribosomes (30S *E.coli* and 50S *T.aq.*) with *in vitro* reconstituted ribosomes carrying the 23S rRNA wild type (wt) T7 transcript. *In vitro* translation of ErmCL was carried out in the presence or absence of the macrolide RU66252 as indicated. Ribosomal stalling was analyzed by the toeprint assay. Reactions were analyzed on a sequencing gel along with dideoxy-sequencing reactions (C, U, A, G). The sequence of *ermCL* is shown along with the sequencing gel and the site of toeprint is indicated by arrows. The isoleucine 9 codon, positioned in the P-site of the stalled ribosome, is boxed. The primer extension stops corresponding to ribosomes occupying the AUG start codon and to the location of the stop codon are indicated by filled arrowheads. The locations of the radiolabeled primer as well as the full length reverse transcription product are highlighted as well. (**B**) Toeprint assay comparing reconstituted ribosomes carrying the wt 23S rRNA *in vitro* transcript to ribosomes harboring a 23S rRNA with deleted residue A2602 (Δ2602). *In vitro* translation was performed either in the presence of RU66252 or mupirocin (Mup). Mupirocin inhibits Ile-tRNA synthetase, leading to accumulation of ribosomes with an empty A-Site (Ile codon) and was used as translation control. In the presence of mupirocin ribosomes arrest translation at Il3 or Ile6 in the A-site, respectively (open arrowheads). Filled arrowheads mark the position of the start codon toeprint and the location of the stop codon, respectively. Reverse transcription analyses of two independent stalling experiments are shown. In total this particular stalling experiment was repeated 6 times. See Supplementary Figure S3 for uncropped gels. (**C**) The chemical structures of the semi-synthetic macrolides RU66252 and solithromycin (both used in this study) and erythromycin, from which they derive. Solithromycin lacks the C3 cladinose sugar and thus is not active in *ermCL* stalling (17). RU66252 does carry a C3 cladinose and has in addition an extended alkyl-aryl side chain attached at the C11 and C12 atoms. These features of RU66252 turned out to be superior for *ermCL* stalling compared to erythromycin in this experimental system.

nucleotide A2602 (Figure 2B), which is in line with previous results demonstrating compromised termination rates of ribosomes lacking this adenosine (33–35).

Sensing of the translation arrest signal involves A2062

The highly conserved A2062 is located in the upper part of the nascent peptide exit tunnel and is one of the most flexible 23S rRNA nucleotides in this region of the large ribosomal subunit (36). Mutation of this residue has been shown to abolish ribosomal stalling on *ermCL* (16). In the cryo-EM structure of the SRC A2062 is found in a distinct conformation, folded flat against the exit tunnel wall and potentially forming a hydrogen bonding interaction with A2503 (Figure 3A) (18). Here, we used the atomic mutagenesis approach to introduce specific modifications either at A2062 or A2503 that disrupt the suggested hydrogen bonding interactions between these two residues (16,18). In order to incorporate modified bases at position A2062, we used a circularly permuted (cp) 23S rRNA containing a short sequence gap around this position. The sequence gap in the 23S rRNA was complemented during *in vitro* reconstitution by a synthetic RNA oligonucleotide carrying either the wild-type (wt) sequence or a nucleoside analog at posi-

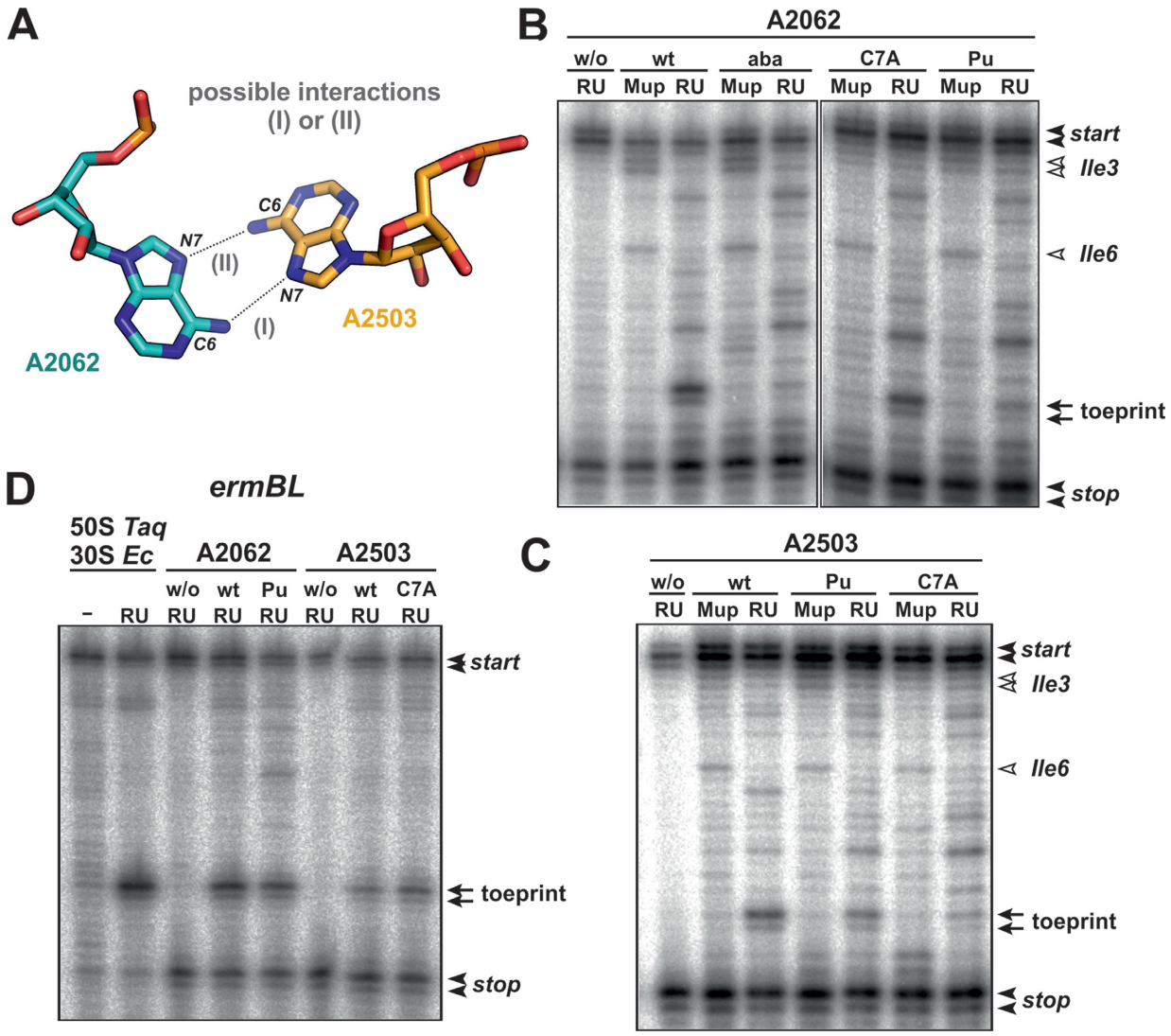

Figure 3. Interaction of A2062 with A2503 is crucial for induced ribosomal arrest on *ermCL*. (**A**) Two possible interactions of 23S rRNA residues A2062 and A2503 based on the structure of the ErmCL stalled ribosomal complex (pdb 3J7Z) (18). The exocyclic C6 amino group of A2062 might form a hydrogen bond with N7 of A2503 (possible interaction I). Alternatively, N7 of A2062 might interact via hydrogen bonding with the C6 exocyclic amino group of A2503 (possible interaction II). (**B**) Toeprint analysis of *in vitro* reconstituted ribosomes, carrying different modifications at position A2062, either in the presence of RU66252 (RU) or in the presence of mupirocin (Mup). Toeprint bands resulting from macrolide induced translational arrest are highlighted by arrows, bands originating from depletion of aminoacylated Ile-tRNA^{Ile} by open arrowheads. Filled arrowheads mark the position of the start codon toeprint and the location of the stop codon, respectively. This particular stalling experiment was repeated 4–7 times. aba: abasic site analog, C7A: 7-deaza-adenosine, Pu: purine nucleobase analog. (**C**) Toeprinting analysis with ribosomes carrying nucleoside modifications at position 2503. All abbreviations as in (B). This particular stalling experiment was repeated 4–10 times. (**D**) Ribosomes containing non-natural nucleoside analogs at positions 2062 or 2503 were used in a toeprint assay to detect ribosomal stalling on *ermBL*. Stalling on *ermBL* occurs with the asparagine codon at position 10 in the P-site. Toeprint bands are indicated by solid arrows. This particular stalling experiment was repeated twice. See Supplementary Figure S4 for uncropped gels.

tion 2062 (see Supplementary Figure S1 for all cp23S rRNA constructs used). When we removed the whole 2062 nucleobase by introduction of an abasic site, the ribosomes were still actively translating as shown by the mupirocin control and the toeprint bands at Ile 3 and 6 (Figure 3B). Ribosomes with an abasic site at A2062 were furthermore fully active in translating a control full-length protein, namely ribosomal protein L12 (Figure 4). However, removal of the nucleobase rendered ribosomes inactive in specific translation arrest at Ile9 in the presence of the macrolide. To test more specifically the suggested interaction with A2503 and the relay pathway (Figure 3A), we either replaced the N7 of the nucleobase of A2062 with a carbon by the introduction of a 7-deaza-adenosine (C7A) or removed its C6 exocyclic amino group, by placing a purine at position 2062 (Figure 1C). Both modifications did not affect general *in vitro* translation activity of these ribosomes as shown in the mupirocin control (Figure 3B). However, removal of the C6 exocyclic amino group by placing the purine nucleoside analog drastically interfered with ribosomal stalling on *ermCL*, whereas removing the H-bond acceptor at the N7 position by introducing 7-deaza-adenosine showed no effect (Figure 3B).

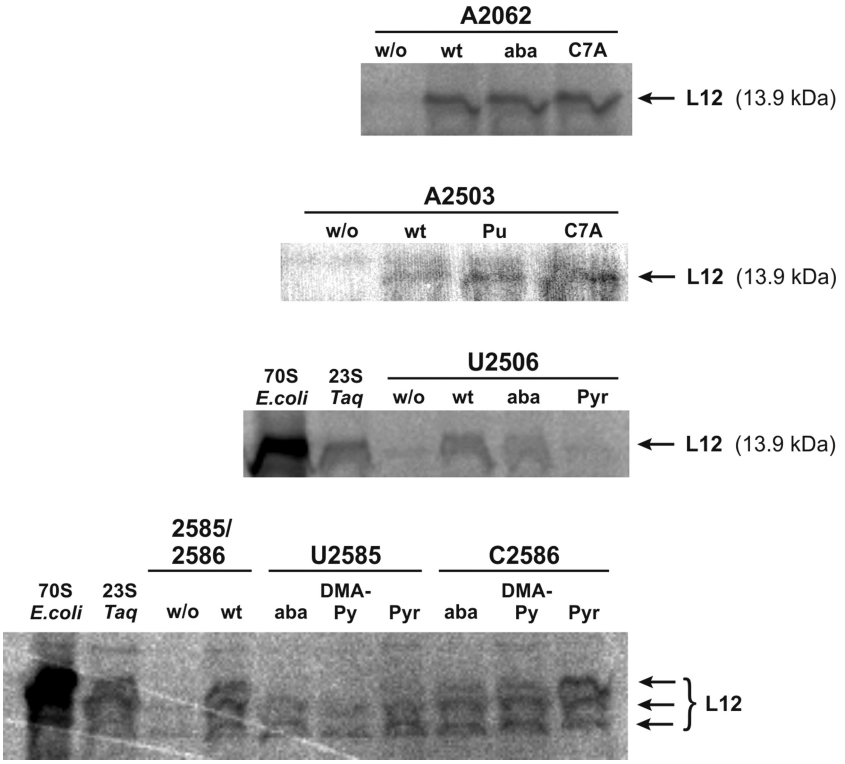

Figure 4. *In vitro* translation activity of ribosomes composed of reconstituted 50S subunits and native *E. coli* 30S subunits. In all cases the mRNA coding for ribosomal protein L12 from *Methanococcus thermolithotrophicus* was used and the [^{35}S]-labeled translation products were detected by exposing the SDS gels to phosphorimager screens (20). The reconstituted 50S either contained full length 23S rRNA *in vitro* transcripts (23S Taq), a cp-23S rRNA without compensating synthetic RNA oligo (w/o), or cp-23S rRNA with RNA oligos encoding the wild type sequence (wt) or harboring nucleoside modifications (see Figure 1C for details). As positive control native *E. coli* 70S ribosomes were used. The faint L12 products sometimes seen in the negative control reactions without compensating RNA oligos (w/o) originate from minor 50S contaminations of the 30S subunit preparation. Note that for unknown reasons in the reaction shown in the lowest panel, multiple translation product bands appeared. These bands likely represent truncated L12 r-proteins that are nevertheless translation products of the chemically engineered ribosomes.

From this we conclude that the functional group of A2062, crucial for sensing and likely signaling of the translation arrest, is the exocyclic NH_2-group at position C6 of the adenine nucleobase.

Interaction of A2062 with A2503 is crucial for ribosome stalling on *ermCL*

In order to further characterize the suggested interaction between A2062 and A2503, we introduced the reciprocal nucleobase modifications at A2503 in order to test possible hydrogen bonding contacts. Ribosomes carrying a purine at position 2503, and thus lacking the hydrogen bond donor functionality of the C6 exocyclic group of the nucleobase, were actively translating as demonstrated in the mupirocin and L12 mRNA translation controls (Figures 3C and 4). Importantly, ribosomes with a purine at 23S rRNA position 2503 still efficiently stall in the presence of the macrolide upon synthesis of ErmCL (Figure 3C). In contrast, when the 7-deaza-adenosine nucleoside analog was introduced at position 2503, drug-dependent translation arrest was strongly impaired, even though these ribosomes were still capable of actively synthesizing proteins (Figures 3C and 4). These data show that the N7 of A2503 is involved in an interaction that is important for establishing the translation arrest. Therefore, the obtained atomic mutagenesis data are compatible with the view that the crucial interaction between 23S rRNA residues 2062 and 2503 takes place between the N7 of A2503 and the NH_2-group at position C6 of A2062 (Figure 3A; possible interaction I).

The A2062-A2503 interaction is not involved in stalling on *ermBL*

After having shown the crucial roles of specific functional groups at A2503 and A2062 for ribosomal stalling on *ermCL*, we next investigated the specificity of these findings. Therefore, we tested ribosomes carrying a purine at 2062 or a C7A at 2503 for their ability to arrest translation upon synthesis of another stalling peptide, ErmBL. It has been shown before that stalling sequences can be arranged into groups according to their dependency on residues A2062 and A2503 for translation arrest (16). The first group includes ErmCL, ErmAL1 and SecM that strictly depend on these two adenine residues. However, the mutations at either A2062 or A2503 did not abolish stalling at *ermBL, ermDL* and *tnaC* regulatory genes (16). In support of these previous data, ribosomes modified at position 2503 (C7A) or 2062 (purine), modifications that abolished stalling on *ermCL*, efficiently arrested translation on *ermBL* in the presence of the macrolide RU66252 (Figure 3D). This highlights the highly specific roles of A2503 and A2062 for ErmCL

stalling. Furthermore, these findings also demonstrate that the abolished stalling for ribosomes with 2503 C7A or 2062 purine modifications during *ermCL* translation is not the result of diminished macrolide binding. These findings suggest that different relay pathways operate for recognizing ErmCL and ErmBL stalling peptides and transmitting the stalling signal from the ribosomal exit tunnel to the PTC.

U2506 contributes to ribosome stalling

In the cryo-EM structure of the ErmCL SRC, density for a putative interaction has been observed of U2506 with F7 and V8 of ErmCL. The nucleobase of U2506 stacks on F7, whereas the C4 carbonyl might interact with V8. As F7 and V8 are part of the essential $I_6F_7V_8I_9$ stalling motif of ErmCL this observed interaction might be important, but its functionality has yet to be biochemically validated. Therefore, to investigate the possible role of the F7/F8 interaction with U2506 on stalling, we first removed the entire nucleobase at position 2506, which resulted in abolished stalling, whereas translation activity was only mildly affected (Figures 5A and 4). In order to understand this interaction in more detail, we removed the carbonyl group at the C4 position of uracil (and concomitantly the N3) by introducing a 2-pyridone analog (Figure 1C). This ablation is expected to disrupt the U2506–V8 interaction. Unexpectedly, ribosomes carrying a 2-pyridone at position 2506 lost the capability for *in vitro* translation (Figure 4). This is the first nucleobase modification of an active site residue that completely abolished translation activities (1,20). Due to this lack of activity we could not further evaluate the role of the C4 carbonyl group for ribosome stalling. Our data nevertheless highlight the importance of the proposed interaction of the 2506 nucleobase with amino acids F7 and V8 of ErmCL for macrolide dependent ribosome stalling.

2585 and 2586

In *E. coli* the highly conserved U2585 and U2586 have been connected with translation arrest. The structure of the ErmCL SRC showed U2585 in a very distinct conformation, as it is flipped out by 80° compared to the unaccommodated state (18). Importantly the C4 carbonyl oxygen of U2585 is in hydrogen bonding distance to the A76 ribose 2′ OH-group of the A-site tRNA during binding and accommodation. In the flipped out conformation of U2585 observed in the ErmCL-stalled complex this interaction cannot be established, which led to the proposal that reorientation of U2585 accounts for the weak A-site tRNA binding for the ErmCL SRC (18). In order to evaluate the role of U2585 in translation arrest on ErmCL we first removed the entire nucleobase. Translational activity of these modified ribosomes was somewhat decreased (Figure 4), however these ribosomes were still able to stall on *ermCL* (Figure 5B). To analyze the contribution of U2585 more closely we eliminated its C4 carbonyl oxygen (and simultaneously also replaced the N3 with a carbon) by incorporation of a 2-pyridone (Figure 1C). Translational activity of these ribosomes was slightly impaired (Figure 4), however they retained their ability to arrest translation, albeit less efficiently compared to the wt construct (Figure 5B). The reduced activity in the stalling assay is therefore attributed to the decreased overall translational activity. However, when we instead replaced the C4 carbonyl with a dimethyl-amino group (Figure 1C), the picture changed. Despite the residual translation activity of these ribosomes (Figure 4), we could not detect any stalling on *ermCL* in the presence of the macrolide RU66252 (Figure 5B). The fact that removal of the whole nucleobase still allows stalling, whereas the 4-dimethyl-amino-pyrimidine does not, might be explained by the bulkiness of the two additional methyl groups at C4 of the pyrimidine nucleobase analog which likely interferes sterically with the stalling reaction. From these data we conclude that nucleobase modification at U2585 primarily decreases translation activity, probably because in all modifications the C4 carbonyl oxygen is lacking and therefore the proposed interaction with the A76 ribose 2′ OH-group of the A-tRNA cannot be established. Besides these defects in overall translation, nucleobase modifications of U2585 (except 4-dimethyl-amino-pyrimidine) did not interfere with translation arrest on *ermCL*. It follows that U2585 plays an important role in translational activities, however, it is not particularly critical for macrolide-dependent ribosomal stalling on *ermCL*.

A different picture emerged when we introduced the same set of modifications as described above at position 2586. While *E. coli* carries a uracil at this position, *T. aquaticus* ribosomes have C2586. Based on the cryo-EM structure of the ErmCL SRC, U2586 has been suggested to interact with the crucial Ile6 of ErmCL (18). Ribosomes carrying an abasic site at 2586 were only slightly hampered in their ability to synthesize proteins. Ribosomes carrying either a 2-pyridone or a 4-dimethyl-amino-pyrimidine at 2586 showed translational activity comparable to the wt control (Figure 4). Despite being active in translation, ribosomes harboring modified nucleoside analogs at 2586 failed to stall on *ermCL* in the presence of the macrolide antibiotic (Figure 5B). This suggests that the crucial interaction from 23S rRNA residue 2586 with the ErmCL nascent peptide chain is executed likely via the C4 exocyclic group (or alternatively *via* its N3). To validate that C2586 base modifications do not affect macrolide binding, and thus would affect *ermCL* stalling indirectly, we performed RU66252 footprinting experiments with reconstituted *T. aquaticus* 50S subunits. It turned out that the characteristic macrolide footprints at 23S rRNA positions A2058/A2059 (37) were unaffected by the introduced base modifications at C2586 (Figure 5C). These data demonstrate that the failure of ribosomes carrying base modifications at 2586 to stall at the *ermCL* ORF is not the consequence of diminished macrolide antibiotic binding. Altogether, our results suggest that the nucleobase of U2585 is required for proper translation activity but is dispensable for translation arrest on *ermCL*. On the other hand, the nucleobase of 2586 does not impact much overall translation, while its C4 exocyclic group is essential for induced ribosomal stalling.

DISCUSSION

In order to specifically arrest translation upon synthesis of the ErmC leader peptide (ErmCL) in a macrolide-dependent manner, specific interactions of nascent chain residues with 23S rRNA tunnel nucleotides are required.

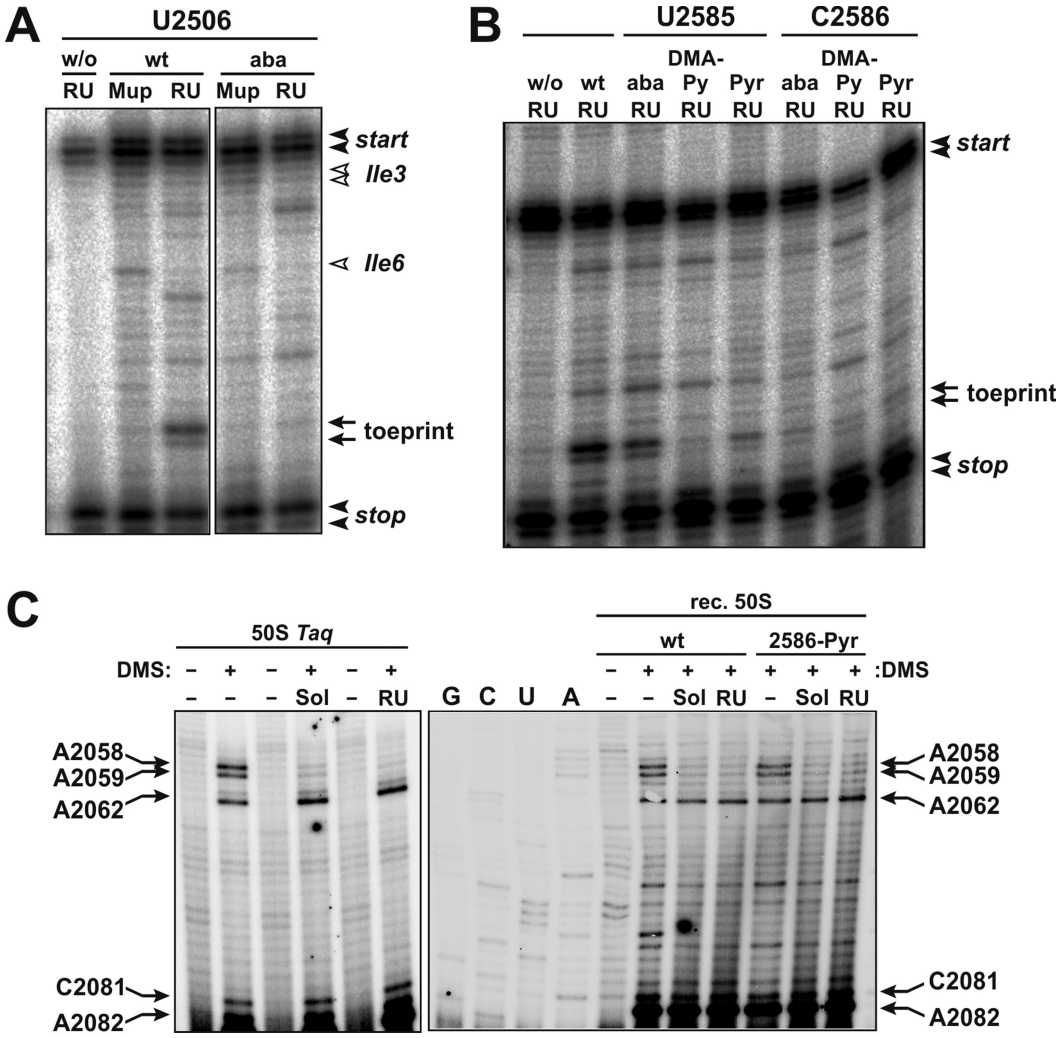

Figure 5. Role of the rRNA residues 2506, 2585 and 2586 in ribosomal stalling on *ermCL*. (**A**) Toeprint analysis using *in vitro* reconstituted ribosomes to characterize the contribution of U2506. *In vitro* translation has been performed in the presence of RU66252 (RU) to analyze their ability to stall at the ninth codon position in the P-site. Reactions in the presence of mupirocin (Mup) served as translation controls. Toeprint bands resulting from macrolide-induced translational arrest are highlighted by arrows, while bands originating from depletion of aminoacylated Ile-tRNA are shown with open arrowheads. Filled arrowheads mark the position of the start codon toeprint and the location of the stop codon, respectively. This particular stalling experiment was repeated six times. (**B**) Ribosomes carrying different modifications either at position 2585 or 2586 were used in the toeprint assay to monitor effects on ribosomal stalling in the presence of RU66252 (RU). *In vitro* reconstituted 50S subunits carrying no compensating synthetic RNA oligonucleotide (w/o) or the unmodified synthetic RNA fragment (wt) served as negative and positive stalling controls, respectively. This particular stalling experiment was repeated four times. Abbreviations used: aba: abasic site analog, Pyr: 2-pyridone, DMA-Py: 4-dimethylamino-pyrimidine. See Supplementary Figure S5 for uncropped gels. (**C**) The DMS reactivities of residues A2058/A2059 in the absence (–) or presence of the macrolides solithromycin (Sol) or RU66252 (RU) was used to monitor binding efficiencies of the antibiotics to native 50S particles (left gel) or reconstituted 50S subunits (right gel). Other DMS reactive residues that do not change modification efficiencies upon macrolide binding and that are similar in native as well as reconstituted 50 S subunits are highlighted as well. G, C, U, A denote dideoxy sequencing reactions. Note that the reverse transcriptase always stops one nucleotide 3′ of the actually methylated nucleobase.

Putatively crucial interactions have been identified by the cryo-EM structure of the ErmCL SRC and by mutational analysis of 23S rRNA nucleotides in the exit tunnel (16,18). Here, we applied the atomic mutagenesis approach (20) to unravel functionally critical 23S rRNA residues in the nascent peptide exit tunnel and in the PTC for macrolide-dependent ribosome stalling. This nucleotide analogue interference method allows studying the functional consequences of single functional group replacements of 23S rRNA nucleosides in the context of *in vitro* assembled 70S ribosomes. Beside obvious advantages of this experimental approach, it is known that the overall reconstitution efficiency is rather low and the obtained ribosomes possess reduced reaction kinetics (23). Therefore we primarily interpreted the apparent stalling efficiencies on a qualitative rather than quantitative level. To compensate for these limitations of the experimental system we always compared results obtained with ribosomes originating from the same set of parallel 50S subunit reconstitutions and repeated each stalling experiment multiple times (see the corresponding figure legends for details). Our study revealed that *in vitro* reconstituted ribosomes are indeed capable of programmed

translational arrest which is a clearly more demanding activity compared to forging single peptide bonds (21), activating translational GTPases (22,38), or translating homopolymeric mRNA analogs (25,30). In order to function during macrolide-dependent ribosome stalling the reconstituted and chemically modified ribosomes not only need to be active in translation of a heteropolymeric mRNA, but also need to sense the stalling signal of the nascent peptide and the antibiotic molecule within the exit tunnel and transmit it back to the PTC (Figures 1A and 2A). In line with our previous observations (25,30), most of the introduced modifications at the different 23S rRNA positions did not interfere with overall translation activity. Importantly not all introduced 23S rRNA modifications on PTC or exit tunnel residues abolished stalling on *ermCL*. For example complete deletion of the universally conserved A2602 or ablation of the nucleobase at U2585 did not eliminate the ribosome's ability to respond to the presence of macrolides by arresting translation of the *ermCL* ORF (Figures 2B and 5B). These findings highlight the principle applicability of chemically engineered ribosomes generated by atomic mutagenesis to functionally pinpoint crucial 23S rRNA groups for drug-dependent ribosome stalling.

Our data unravel important roles for two adenine nucleobases at positions 2503 and 2062 in the nascent peptide exit tunnel for ribosome stalling. In particular the N7 nitrogen at A2503 and the C6 exocyclic amino group at A2062 turned out to be crucial for ErmCL-dependent translation arrest (Figure 3). While replacement of a single heteroatom (the N7 nitrogen by a carbon) or the ablation of the C6 amino group at A2503 and A2062, respectively, did not eliminate overall protein synthesis (Figure 4), it completely destroyed the macrolide-dependent ribosome stalling potential on the *ermCL* ORF (Figure 3B). The findings of unaffected activities in protein biosynthesis, as revealed by the *in vitro* translation data (Figure 4) and the mupirocin controls (Figure 3B and C), make potential peptidyl-tRNA drop-off as the cause for the lack of ribosome stalling unlikely. Importantly, the very same nucleobase groups at A2503 and A2062 are not critical for stalling on the ErmBL nascent chain (Figure 3D). This demonstrates that these chemically engineered ribosomes retain their general activity for sensing the nascent peptide inside the exit tunnel, and points to amino acid specific roles of A2503 and A2062 during the ErmCL-mediated arrest. Based on these findings we suggest that in order to establish a precise translation arrest within the *ermCL* ORF, the N7 of A2503 interacts with the C6 exocyclic amino-group of A2062 likely *via* hydrogen bonding (Figure 3A; possible interaction I). This interpretation is compatible with genetic data showing that the adenines at 2503 and 2062 are critically involved in translational arrest on *ermCL* (16). Also recent structural data emphasize a crucial role of these nucleotides since it has been suggested that the N-terminus of ErmCL forces the otherwise highly flexible A2062 in a distinct conformation flat against the tunnel wall (18). Only in this constrained conformation, the specific interaction with A2503 can be established.

While the roles of the nascent peptide chain, certain rRNA residues in the tunnel wall and a ribosome-bound macrolide in programmed translation arrest at *ermCL* has been largely established, the means by which the stalling signal is transmitted from the tunnel to the PTC is still unclear. Basically there are two options: either the signal is transmitted via the nascent polypeptide chain (18) or via 23S rRNA residues (17). Our data are fully compatible with the latter scenario since A2062 is flanked by G2061 and C2063. Both of these nucleosides belong to the outer shell of the PTC and participate in positioning of A2451, the key catalytic residue in the active site (4,35,39,40). Therefore A2062 seems to be perfectly located to sense the nascent polypeptide chain and communicate the stalling signal to the PTC. The crucial role of A2503 and A2062 for signal transmission was also emphasized by molecular dynamics simulations (41). A2062 is universally conserved and highly flexible (42). Importantly, also the mobility of this residue seems to be highly conserved suggesting that the ribosome requires this flexibility for its proper functioning. Unexpectedly, complete elimination of the entire nucleobase at 2062 had essentially no effect on *in vitro* protein synthesis (Figure 4 and ref. 25) indicating a more elaborate role of the adenine base. Indeed, here we show that the highly flexible A2062 is required for fine-tuning protein synthesis, namely for sensing the regulatory nascent peptide chain for macrolide-induced ribosomal stalling upon synthesis of ErmCL. The crucial coplayer of A2062 in ribosomal stalling is the highly conserved A2503. A2503 is one of the few posttranscriptionally modified rRNA residue in *E. coli* and other bacteria carrying a C2 methyl group. It has been shown that posttranscriptional modification of A2503 affects the ability of the ribosome to stall upon synthesis of ErmCL (16). However, in our experimental system, which depends on *in vitro* transcripts of 23S rRNA, A2503 is unmodified, yet the ribosomes are still capable of establishing the canonical stalling complex (Figure 2A).

Besides A2503/A2062 other residues were also identified to contribute to ribosome stalling. U2585 and U2586 contact the nascent ErmCL in the exit tunnel (18). All of the nucleobase modifications tested at U2585 markedly reduced the ribosomes ability to translate heteroploymeric mRNA (Figure 4), whereas they were fully active in the puromycin reaction and in poly(U) translation (23,25). Importantly, none of the introduced nucleobase modifications at U2585 possess a C4 carbonyl oxygen or a group with similar chemical properties (Figure 1C). This might lead to an impaired A-site tRNA accommodation efficiency as suggested by others (18,43–45). Significantly, even though we observed a clear decrease in translation activity when replacing the uridine at 2585 by an abasic site analog or by the 2-pyridone nucleoside, those ribosomes were still able to stall at the expected site on the *ermCL* ORF (Figure 5B). These data indicate that the nucleobase at U2585 contributes to overall translation activity, however is not required for ribosomal stalling. In clear contrast to these findings are the results obtained for nucleobase modifications at the neighboring position 2586. Although translation activity was slightly decreased, we could still observe substantial translation products (Figure 4). However, all of the nucleobase modifications introduced at 2586 severely interfered with ribosomal stalling on *ermCL*, emphasizing the importance of this residue for translation arrest. These results are supported by structural data, showing U2586 in close proximity to Ile6 of the ErmCL nascent peptide (18). Ile6 is one

of the amino acids that are crucial for *ermCL* stalling as its mutation to alanine completely abolishes stalling (17). Interestingly, mutation of U2586 (to either A, C or G) does not eradicate stalling, but can partially restore stalling of the I6A-ErmCL mutant (18). In these standard mutagenesis experiments (18), all 2586 mutants retained a C4 or C6 exocyclic group with free electron pairs and thus hydrogen bond acceptor capabilities. However in our atomic mutagenesis approach we completely removed or significantly disturbed this hydrogen bond acceptor functionality by removing either the entire nucleobase, or by the ablation of the C4 exocyclic group, or by placing a bulky C4 dimethylamino group. Our observations are compatible with two scenarios: (i) the exocyclic C4 group at position 2586 is needed to form a crucial interaction with Ile6 of the ErmCL (possibly via hydrogen bonding), or (ii) it is required to expand the aromatic π-electron system thus enhancing stacking interactions with Ile6.

In summary, our experiments corroborate and expand previous conclusions suggesting crucial roles for the 23S rRNA residues A2062, A2503 and U2586 (*E. coli* nomenclature) for translation arrest on *ermCL*, but not on *ermBL*. By utilizing the power of the atomic mutagenesis approach we could unravel important molecular interactions for ribosome stalling in more detail. The results on A2062 and A2503 strongly suggest that the interaction between these two nucleobases is established via the C6 exocyclic amino group of A2062 and the N7 of A2503. Those adenosines are universally conserved, yet they do not contribute pivotally to overall translation. This indicates that their evolutionary sequence constraint originates from functional roles that go beyond mere protein biosynthesis. We believe that the intra-ribosomal A2062/A2503-dependent signal transmission activity might represent such an elaborate role for these two 23S rRNA residues.

SUPPLEMENTARY DATA

Supplementary Data are available at NAR Online.

ACKNOWLEDGEMENTS

We thank Alexander Mankin, Nora Vazquez-Laslop, and Matthias Erlacher for critical comments on the manuscript. We are especially gratefully to Alexander Mankin for providing antibiotics and the entire Mankin lab for initial experimental help with the toeprinting assay. Our thanks are extended to Christian Berk and Mauro Zimmermann for help with the synthesis of oligoribonucleotides.

FUNDING

NCCR 'RNA & Disease' funded by the Swiss National Science Foundation; Swiss National Science Foundation [31003A_166527 to N.P.]. Funding for open access charge: NCCR 'RNA & Disease' funded by the Swiss National Science Foundation.
Conflict of interest statement. None declared.

REFERENCES

1. Erlacher,M.D. and Polacek,N. (2008) Ribosomal catalysis: the evolution of mechanistic concepts for peptide bond formation and peptidyl-tRNA hydrolysis. *RNA Biol.*, **5**, 5–12.
2. Polacek,N. and Mankin,A.S. (2005) The ribosomal peptidyl transferase center: structure, function, evolution, inhibition. *Crit. Rev. Biochem. Mol.*, **40**, 285–311.
3. Ban,N., Nissen,P., Hansen,J., Moore,P.B. and Steitz,T.A. (2000) The complete atomic structure of the large ribosomal subunit at 2.4 A resolution. *Science*, **289**, 905–920.
4. Nissen,P., Hansen,J., Ban,N., Moore,P.B. and Steitz,T.A. (2000) The structural basis of ribosome activity in peptide bond synthesis. *Science*, **289**, 920–930.
5. Harms,J., Schluenzen,F., Zarivach,R., Bashan,A., Gat,S., Agmon,I., Bartels,H., Franceschi,F. and Yonath,A. (2001) High resolution structure of the large ribosomal subunit from a mesophilic eubacterium. *Cell*, **107**, 679–688.
6. Schuwirth,B.S., Borovinskaya,M.A., Hau,C.W., Zhang,W., Vila-Sanjurjo,A., Holton,J.M. and Cate,J.H. (2005) Structures of the bacterial ribosome at 3.5 A resolution. *Science*, **310**, 827–834.
7. Selmer,M., Dunham,C.M., Murphy,F.V.t., Weixlbaumer,A., Petry,S., Kelley,A.C., Weir,J.R. and Ramakrishnan,V. (2006) Structure of the 70S ribosome complexed with mRNA and tRNA. *Science*, **313**, 1935–1942.
8. Deutsch,C. (2003) The birth of a channel. *Neuron*, **40**, 265–276.
9. Wilson,D.N., Arenz,S. and Beckmann,R. (2016) Translation regulation via nascent polypeptide-mediated ribosome stalling. *Curr. Opin. Struct. Biol.*, **37**, 123–133.
10. Wilson,D.N. and Beckmann,R. (2011) The ribosomal tunnel as a functional environment for nascent polypeptide folding and translational stalling. *Curr. Opin. Struct. Biol.*, **21**, 274–282.
11. Ito,K. and Chiba,S. (2013) Arrest peptides: cis-acting modulators of translation. *Annu. Rev. Biochem.*, **82**, 171–202.
12. Ramu,H., Mankin,A. and Vazquez-Laslop,N. (2009) Programmed drug-dependent ribosome stalling. *Mol. Microbiol.*, **71**, 811–824.
13. Hahn,J., Grandi,G., Gryczan,T.J. and Dubnau,D. (1982) Translational attenuation of ermC: a deletion analysis. *Mol. Gen. Genet.*, **186**, 204–216.
14. Mayford,M. and Weisblum,B. (1989) ErmC leader peptide. Amino acid sequence critical for induction by translational attenuation. *J. Mol. Biol.*, **206**, 69–79.
15. Gupta,P., Liu,B., Klepacki,D., Gupta,V., Schulten,K., Mankin,A.S. and Vazquez-Laslop,N. (2016) Nascent peptide assists the ribosome in recognizing chemically distinct small molecules. *Nat. Chem. Biol.*, **12**, 153–158.
16. Vazquez-Laslop,N., Ramu,H., Klepacki,D., Kannan,K. and Mankin,A.S. (2010) The key function of a conserved and modified rRNA residue in the ribosomal response to the nascent peptide. *EMBO J.*, **29**, 3108–3117.
17. Vazquez-Laslop,N., Thum,C. and Mankin,A.S. (2008) Molecular mechanism of drug-dependent ribosome stalling. *Mol. Cell*, **30**, 190–202.
18. Arenz,S., Meydan,S., Starosta,A.L., Berninghausen,O., Beckmann,R., Vazquez-Laslop,N. and Wilson,D.N. (2014) Drug sensing by the ribosome induces translational arrest via active site perturbation. *Mol. Cell*, **56**, 446–452.
19. Blaha,G., Gurel,G., Schroeder,S.J., Moore,P.B. and Steitz,T.A. (2008) Mutations outside the anisomycin-binding site can make ribosomes drug-resistant. *J. Mol. Biol.*, **379**, 505–519.
20. Erlacher,M.D., Chirkova,A., Voegele,P. and Polacek,N. (2011) Generation of chemically engineered ribosomes for atomic mutagenesis studies on protein biosynthesis. *Nat. Protoc.*, **6**, 580–592.
21. Erlacher,M.D., Lang,K., Shankaran,N., Wotzel,B., Huttenhofer,A., Micura,R., Mankin,A.S. and Polacek,N. (2005) Chemical engineering of the peptidyl transferase center reveals an important role of the 2′-hydroxyl group of A2451. *Nucleic Acids Res.*, **33**, 1618–1627.
22. Koch,M., Flur,S., Kreutz,C., Ennifar,E., Micura,R. and Polacek,N. (2015) Role of a ribosomal RNA phosphate oxygen during the EF-G-triggered GTP hydrolysis. *Proc. Natl. Acad. Sci. U.S.A.*, **112**, E2561–2568.
23. Erlacher,M.D., Lang,K., Wotzel,B., Rieder,R., Micura,R. and Polacek,N. (2006) Efficient ribosomal peptidyl transfer critically relies

on the presence of the ribose 2′-OH at A2451 of 23S rRNA. *J. Am. Chem. Soc.*, **128**, 4453–4459.
24. Khaitovich,P. and Mankin,A.S. (1999) Effect of antibiotics on large ribosomal subunit assembly reveals possible function of 5S rRNA. *J. Mol. Biol.*, **291**, 1025–1034.
25. Chirkova,A., Erlacher,M.D., Clementi,N., Zywicki,M., Aigner,M. and Polacek,N. (2010) The role of the universally conserved A2450-C2063 base pair in the ribosomal peptidyl transferase center. *Nucleic Acids Res.*, **38**, 4844–4855.
26. Erlacher,M.D. and Polacek,N. (2012) Probing functions of the ribosomal peptidyl transferase center by nucleotide analog interference. *Methods Mol. Biol.*, **848**, 215–226.
27. Pradere,U., Brunschweiger,A., Gebert,L.F., Lucic,M., Roos,M. and Hall,J. (2013) Chemical synthesis of mono- and bis-labeled pre-microRNAs. *Angew. Chem. Int. Ed. Engl.*, **52**, 12028–12032.
28. Guennewig,B., Stoltz,M., Menzi,M., Dogar,A.M. and Hall,J. (2012) Properties of N(4)-methylated cytidines in miRNA mimics. *Nucleic Acid Therap.*, **22**, 109–116.
29. Shah,K., Wu,H. and Rana,T.M. (1994) Synthesis of uridine phosphoramidite analogs: reagents for site-specific incorporation of photoreactive sites into RNA sequences. *Bioconjug. Chem.*, **5**, 508–512.
30. Koch,M., Clementi,N., Rusca,N., Vogele,P., Erlacher,M. and Polacek,N. (2015) The integrity of the G2421-C2395 base pair in the ribosomal E-site is crucial for protein synthesis. *RNA Biol.*, **12**, 70–81.
31. Polacek,N. and Barta,A. (1998) Metal ion probing of rRNAs: evidence for evolutionarily conserved divalent cation binding pockets. *RNA*, **4**, 1282–1294.
32. Khaitovich,P., Tenson,T., Kloss,P. and Mankin,A.S. (1999) Reconstitution of functionally active Thermus aquaticus large ribosomal subunits with in vitro-transcribed rRNA. *Biochemistry*, **38**, 1780–1788.
33. Amort,M., Wotzel,B., Bakowska-Zywicka,K., Erlacher,M.D., Micura,R. and Polacek,N. (2007) An intact ribose moiety at A2602 of 23S rRNA is key to trigger peptidyl-tRNA hydrolysis during translation termination. *Nucleic Acids Res.*, **35**, 5130–5140.
34. Polacek,N., Gomez,M.G., Ito,K., Nakamura,Y. and Mankin,A.S. (2003) The critical role of the universally conserved A2602 of 23S ribosomal RNA in the release of the nascent peptide during translation termination. *Mol. Cell*, **11**, 103–112.
35. Youngman,E.M., Brunelle,J.L., Kochaniak,A.B. and Green,R. (2004) The active site of the ribosome is composed of two layers of conserved nucleotides with distinct roles in peptide bond formation and peptide release. *Cell*, **117**, 589–599.
36. Fulle,S. and Gohlke,H. (2009) Statics of the ribosomal exit tunnel: implications for cotranslational peptide folding, elongation regulation, and antibiotics binding. *J. Mol. Biol.*, **387**, 502–517.
37. Llano-Sotelo,B., Dunkle,J., Klepacki,D., Zhang,W., Fernandes,P., Cate,J.H. and Mankin,A.S. (2010) Binding and action of CEM-101, a new fluoroketolide antibiotic that inhibits protein synthesis. *Antimicrob. Agents Chemother.*, **54**, 4961–4970.
38. Clementi,N., Chirkova,A., Puffer,B., Micura,R. and Polacek,N. (2010) Atomic mutagenesis reveals A2660 of 23S ribosomal RNA as key to EF-G GTPase activation. *Nat. Chem. Biol.*, **6**, 344–351.
39. Polikanov,Y.S., Steitz,T.A. and Innis,C.A. (2014) A proton wire to couple aminoacyl-tRNA accommodation and peptide-bond formation on the ribosome. *Nat. Struct. Mol. Biol.*, **21**, 787–793.
40. Lang,K., Erlacher,M., Wilson,D.N., Micura,R. and Polacek,N. (2008) The role of 23S ribosomal RNA residue A2451 in peptide bond synthesis revealed by atomic mutagenesis. *Chem. Biol.*, **15**, 485–492.
41. Makarov,G.I., Golovin,A.V., Sumbatyan,N.V. and Bogdanov,A.A. (2015) Molecular Dynamics Investigation of a Mechanism of Allosteric Signal Transmission in Ribosomes. *Biochemistry (Mosc.)*, **80**, 1047–1056.
42. Hansen,J.L., Ippolito,J.A., Ban,N., Nissen,P., Moore,P.B. and Steitz,T.A. (2002) The structures of four macrolide antibiotics bound to the large ribosomal subunit. *Mol. Cell*, **10**, 117–128.
43. Schmeing,T.M., Huang,K.S., Kitchen,D.E., Strobel,S.A. and Steitz,T.A. (2005) Structural insights into the roles of water and the 2′ hydroxyl of the P site tRNA in the peptidyl transferase reaction. *Mol. Cell*, **20**, 437–448.
44. Schmeing,T.M., Huang,K.S., Strobel,S.A. and Steitz,T.A. (2005) An induced-fit mechanism to promote peptide bond formation and exclude hydrolysis of peptidyl-tRNA. *Nature*, **438**, 520–524.
45. Schmeing,T.M., Seila,A.C., Hansen,J.L., Freeborn,B., Soukup,J.K., Scaringe,S.A., Strobel,S.A., Moore,P.B. and Steitz,T.A. (2002) A pre-translocational intermediate in protein synthesis observed in crystals of enzymatically active 50S subunits. *Nat. Struct. Biol.*, **9**, 225–230.